Supplementary information

The amyloid architecture provides a scaffold for enzyme-like catalysts

Z. S. Al-Garawi [a, b], B. A. McIntosh [a,c], D. Neill-Hall [a] A. A. Hatimy [d], S. M. Sweet [d], M. C. Bagley [a], and L. C. Serpell

Supplementary Methods

Peptide characterisation

High performance liquid chromatography
0.1-1.5 mg/mL peptides were dissolved in MeCN: H_2O (1:1), vortexed, centrifuged and then sonicated for 1 min. Degassed solvents of solution A (milli-Q water + 0.1% TFA) and solution B (MeCN + 0.1 % TFA) were used for column equilibration and peptide elution. 100-300 µL of each peptide was injected onto a reversed phase HPLC (JASCO) C18 column (250 mm length*4.6 mm internal diameter* packed with 5 µm particles, Vydac). Peptides were eluted at a flow rate of 1 mL/min with a gradient solution B 30-70% or 5-85% for capped and uncapped peptides, respectively for a 40 min run. The intensity was detected using a UV detector at λ 280 and 210 nm.

Mass spectrometry analysis
Peptide samples were sprayed in a 50% MeCN, 0.1% formic acid solution from an IonMax Source (Thermo), using a flow-rate between 3-10 µl/min and an applied voltage of 3.5-5 kV, into an Orbitrap-XL mass spectrometer (Thermo). High resolution FT-MS data was acquired for precursors. Both FT-MS and LTQ-MS spectra were acquired for fragment ions. Peptide identifications were manually validated, visualising spectra using Xcalibur QualBrowser (v2.1; Thermo).

Supplementary Results

HPLC analysis
The success of microwave solid phase synthesis for each peptide was assessed using HPLC analysis. The majority components of **I**, **II**, **III**, **IV**, **V** and **VI** were eluted at a retention time (Rt) 15.8 min, 12.1 min, 8.5 min, 10.9 min, 15.7 min and 16.9 min, respectively within 40 min run times. The crude peptides were eluted close to the main peak of each peptide of interest. All peptides were analysed using a gradient of 5-85% solution B except peptides **III** and **IV** which were analysed using the gradient 30-70% of solution B.
The purity of each synthesised peptide is shown in Table S1 and Figure S1.

Table S1. The purity of the synthesised peptides indicated by the peak area%.

Peptide	**I**	**II**	**III**	**IV**	**V**	**VI**
Purity%	93.75	92.34	95.28	79.79	95.18	94.18

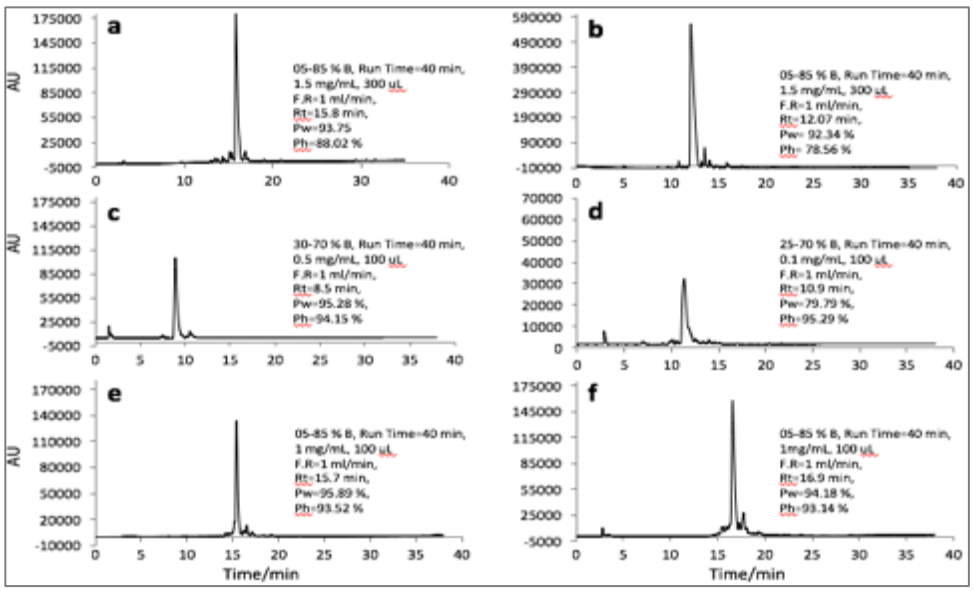

*Figure S1. Reversed-phase High-Performance Liquid chromatographic (RP-HPLC) of the crude peptides **I**, **II**, **III**, **IV**, **V** and **VI** on a C18 column. A linear gradient of 5%- 85% and 30-70%, of solvent B was used. Absorbance at 280 nm is monitored versus Retention time (Rt). The numbers above each peak represent the peak area relative to the entire run time; 40 min. a) peptide **I**, b) peptide **II**, c) peptide **III**, d) peptide **IV**, e) peptide **V** and f) peptide **VI**.*

Mass Spectrometry

Samples were analysed by direct infusion-LC-MS as previously described [1]. The C and N-terminal peptides were detected in double and triple charged forms. The raw MS and MS/MS spectra were converted to mgf format using Compass [2] and searched against the SwissProt database using Mascot (Matrix Science). Search parameters employed a precursor tolerance of 5 ppm and a fragment ion tolerance of 0.6 Da, Figure S2. These double charges numbers refer to the experimental masses of these peptides, which were in agreement with the theoretical mass of the peptides.

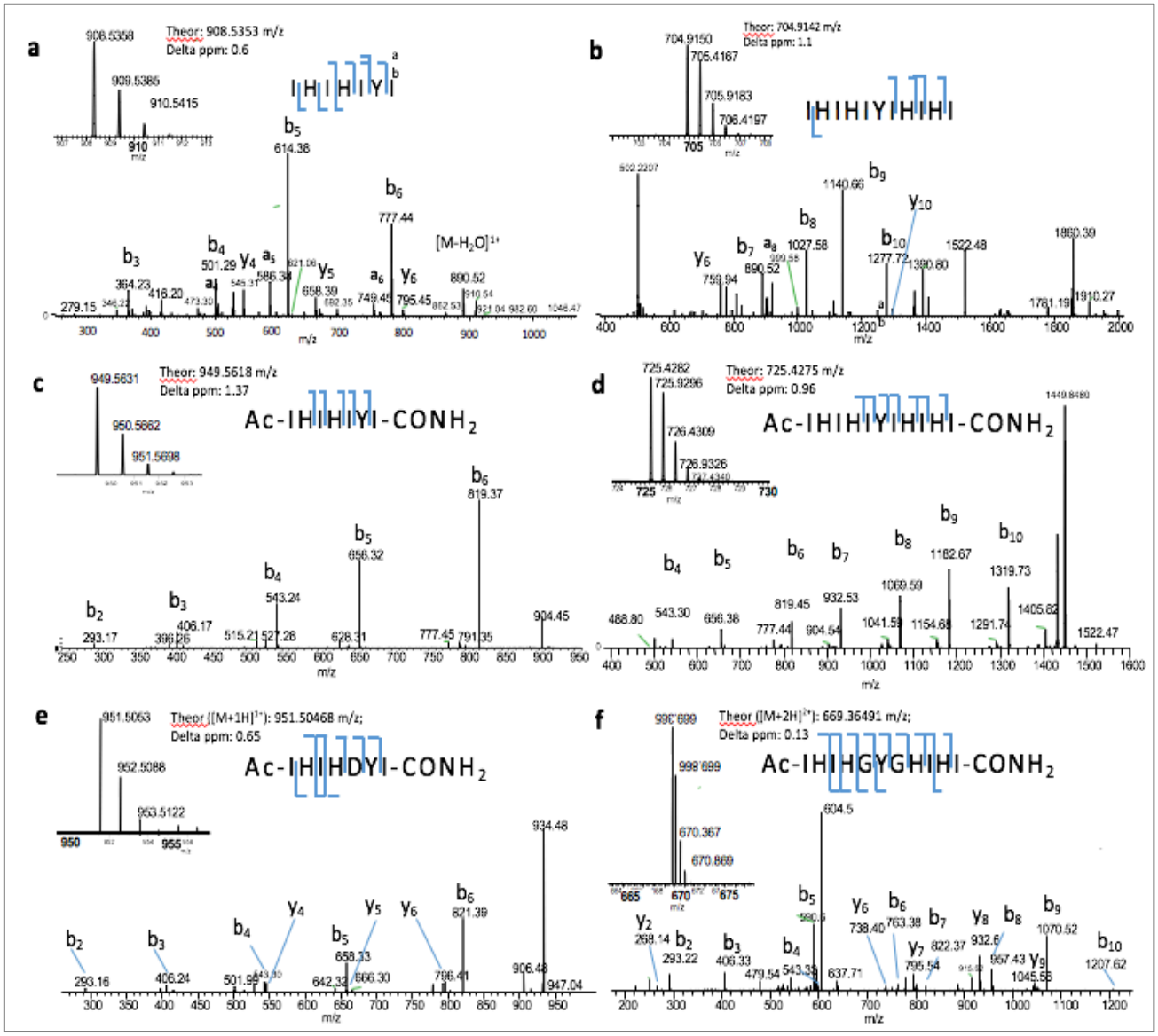

Figure S2. Mass spectrometric analysis of synthetic peptides. High resolution precursor and fragment ion spectra were acquired to confirm peptide identities: ***I*** *(a),* ***II*** *(b),* ***III*** *(c),* ***IV*** *(d),* ***V*** *(e) and* ***VI*** *(f).*

FTIR of peptides **I-VI** confirms β–sheet content as shown in Figure 3.

Table S2 shows the measurement of peaks for each peptide FTIR spectrum.

Table S2. Frequency of IR spectroscopic absorptions[a] for peptide fibrils and their assignments [3].

Peptide	*Amide I* 1700-1600					*Amide II* 1580-1510[b]	*H-Bonding* 3570-3200[b]
	β-sheet 1637-1613[b]	*Parallel* ≈1630[b]	*Anti-parallel* ≈1630/1685[b]	*α-helix* 1662-1645[b]	*Random coil* 1645-1637[b]		
(I)	1630	1630	1630/1669	-	-	1516	3267
(II)	1627	1627	1627/1668	-	-	1540	3268
(III)	1630	1630	Broad ~1670	-	-	1542	3267
(IV)	1630	1630	1630/1667	-	-	1548	3268
(V)	1628	1628	Broad ~1673	-	-	1542	3268
(VI)	1626	1626	1626/1666	-	-	1543	3274

[a] All frequencies are given in cm^{-1}. [b] Reported frequency of absorption of structural units [3].

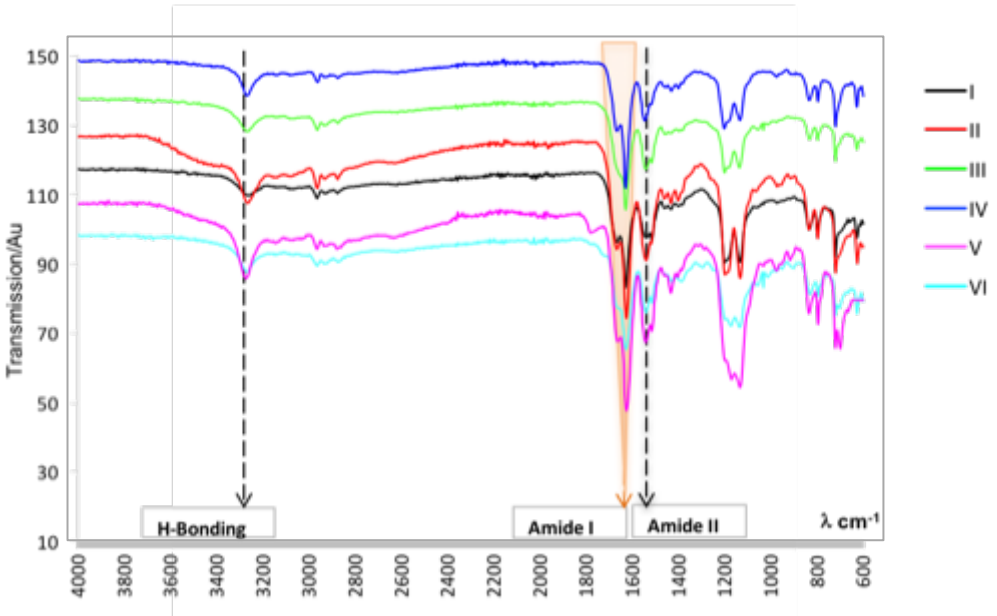

*Figure S3. FTIR spectra of peptides **I-VI**. Broken lines to facilitate indicating the differences between each peptide spectrum.*

X-RFD patterns are shown in Figure 5. The measurement of the positions on reflections is tabulated in Table S3.

Table S3. Diffraction signal positions measured from X-RFD patterns collected from partially aligned fibrils formed by 10 mg/mL solutions of the catalytic peptides (**I-VI**) on third-day fibrillation incubated in water in the absence and presence of Zn^{2+}.

Reflections	***- Zn+2***						***+ Zn+2***					
	I	**II**	**III**	**IV**	**V**	**VI**	**I**	**II**	**III**	**IV**	**V**	**VI**
Meridional												
	4.70	4.70	4.72	4.71	4.70	4.72	4.70	4.70	4.70	4.70	4.70	4.70
				6.5	6.5					6.5		
Off Meridional												
	3.8		3.8	3.8			3.8		3.8			
Equatorial												
	22	23	23	23.0	23.5	24	22.0	23	23	23	24	24
	12	12	12	12	12		12	12	12	12	12	
						11						11
		8	8	8				8	8	8	8	8
		6	6.4	6.5					6	6.5		

Enzyme kinetics measurements are shown in Figure 6. The results from peptides **I**, **II**, **V** (self-assembled with Zn^{2+}) and from peptide **III** without $Zn^{2+}$are shown in Figure S4.

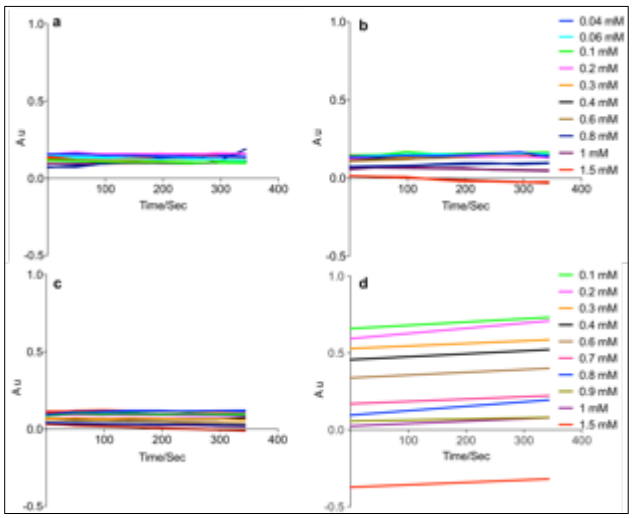

*Figure S4. Linear regression graphics of the catalytic activity without Zn, with uncapped peptides and with peptide **V**. The uncapped **I** (a), peptides **II** (b) and the capped peptide **V** (c) which self-assembled in the presence of Zn^{+2} at 37° C , as well as, capped peptide **III** (d) (self-assembled without Zn^{+2}) were all not able to hydrolyse p-NPA at any considerable level. The substrate concentration range for the uncapped peptides was 0.04-1.5 mM and for the capped peptides was 0.1-1.5 mM.*

The X-ray Fibre diffraction pattern for peptide **III** was examined using CLEARER [4] and a possible unit cell was determined of a=4.7 Å, b=24 Å, c=23 Å, $\alpha=\beta=\gamma=90°$. A model of the sequence for peptide **III** was generated using Pymol [5] and CLEARER [4] was used to calculate a diffraction pattern from the model structure in a fibre architecture. The experimental diffraction pattern is shown with the calculated diffraction pattern as an insert (Figure S5), showing a good match for both parallel and antiparallel arrangements between the β-sheets. It is not possible to distinguish between the two models, and the low number of diffraction signals observed by X-ray fibre diffraction is insufficient for further modelling. The patterns calculated from the models match the experimental diffraction data well and therefore represent possible architectures of peptide **III**. Ss NMR analysis has suggested that the peptides may arrange in a parallel orientation of the β-sheets [6].

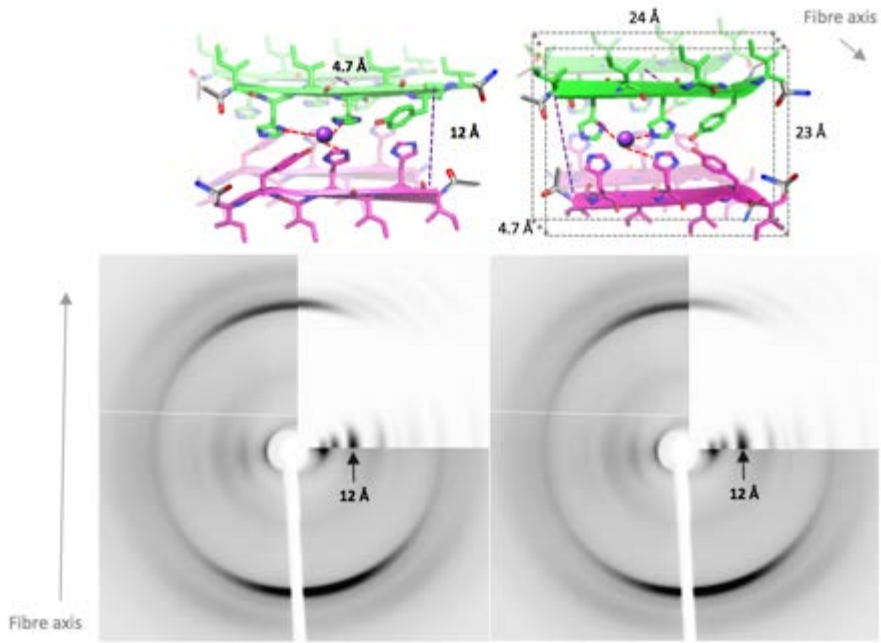

*Figure S5. Model structures and their corresponding diffraction patterns. Top, shows the model structures of peptide **III** that were built into the determined unit cell (shown only on the right-hand model). The diffraction patterns shown below are experimental patterns with inserts showing a quadrant of the patterns calculated from the model structures within the unit cell.*

References

1. A. A. Hatimy, M. J. G. Browne, A. Flaus and S. M. M. Sweet, *International Journal of Mass Spectrometry*, 2015,
2. C. D. Wenger, D. H. Phanstiel, M. V. Lee, D. J. Bailey and J. J. Coon, *Proteomics*, 2011, **11**, 1064-1074.
3. M. Jackson and H. H. Mantsch, *Critical Rev Biochem Mol Biol*, 1995, **30**, 95-120.
4. O. S. Makin, P. Sikorski and L. C. Serpell, *Appl. Cryst.*, 2007, **40**, 966-972.
5. DeLano WL. The PyMOL molecular graphics system. DeLano Scientific, San Carlos, USA; 2002.
6 Lee M, Wang T, Makhlynets OV, Wu Y, Polizzi NF, Wu H, et al. Proceedings of the National Academy of Sciences of the United States of America. 2017,**114**, 6191-6196.